Computational Pathology: TP53 Mutation Status prediction in Lung Adenocarcinoma

Andrew Bell

1 Introduction

In this report, I discuss the process and results of implementing a computational pathology pipeline to predict TP53 mutation status of Lung Adenocarcinoma (LUAD) tumours. I used 100 H&E stained whole slide images (WSIs), as well as the deep features extracted from them at 20x magnification. These WSIs are a subset of the TCGA-LUAD cohort, with 50 being TP53 mutated, and 50 are not mutated (wild type).

2 Tissue Segmentation

Tissue segmentation was performed using TIAToolbox[1], specifically I used WSIReader.tissue_mask() to compute a tissue mask, and to visualise I plotted both the WSI thumbnail and mask thumbnail using Matplotlib. The tissue segmentation results can be seen in figure 1.

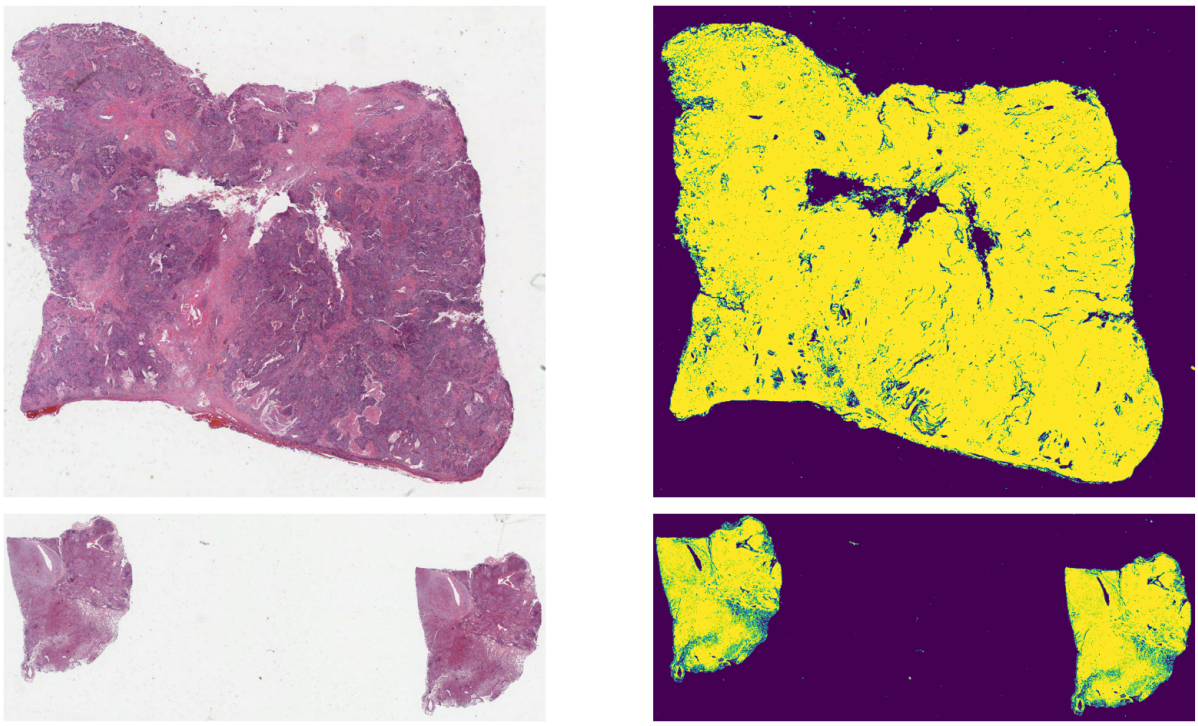

Figure 1: Tissue segmentation results on the two whole-slide images

3 Multiple Instance Learning

Multiple instance learning was performed on the feature bags at 20x magnification, using triplet ranking implemented by TripletMIL [2]. The model itself has two linear layers, with a leaky ReLU activation after the first layer, and a sigmoid activation after the second. The model is illustrated in figure 2. The

key part of this learning framework is the loss function, which penalises intra-class variance for negative samples and rewards inter-class variance between positive and negative samples. This is based on the assumption that negative sample features do not share properties with positive samples, but positive samples exhibit variance amongst themselves. For our task, this means that by using this framework, I assume that wild-type LUAD tumour regions exhibit no features shared by mutated regions. as I did for task 3 The learning hyperparameters I used to train the model are given in table 1. These were left mostly unchanged from the TripletMIL default parameters. The training loss curve can be seen in figure 3. The final area under ROC curve was 0.459. The ROC curve was not plotted, as no real change could be observed. The reason for the low performance is likely the difficulty of predicting TP53 mutation status from visual features.

I used the trained model to predict the mutation status of tissue regions in the WSIs given in the test set. In particular, I perform prediction on the given features for one TP53 mutated LUAD tumour and one wild-type tumour.

Table 1: Learning Hyperparameters

Parameter	Value
Epochs	30
Learning Rate	0.0003
K Ratio	0.1

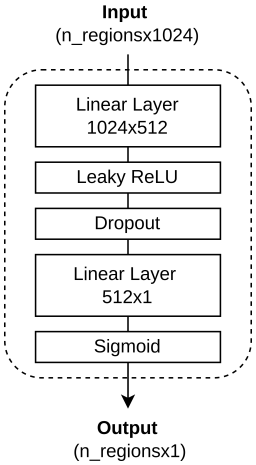

Figure 2: Model Architecture of TripletMIL

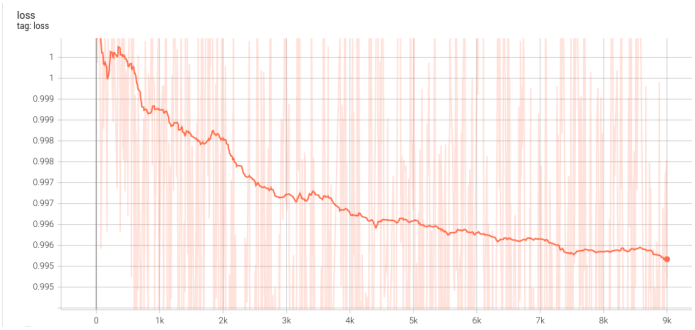

Figure 3: Loss curve of training TripletMIL over 30 epochs

4 Visualising Results

To visualise the results of the prediction, I used the predicted labels for each bag to create a heatmap. This was done by scaling the coordinates of the bag coordinates from 20x magnification to 1x. This means that each coordinate was divided by 20, and used alongside the predicted labels to populate a heatmap of the same size as the WSI thumbnail at 1x magnification. Two examples can be seen in figure 4. The heatmaps were displayed over the WSI thumbnail, to highlight regions that the model identifies with more confidence as being mutated. Finally, I extracted tissue masks, and set all heatmap regions outside of this mask to 0, and set a minimum value of 0.1 for the heatmap display, to ignore these values. This prevented the background of the heatmap displaying on the WSI thumbnail.

I performed this visualisation procedure on two WSIs, one TP53 mutated and one wild type tumour. The results on the two WSIs can be seen in figures 5 and 6. The predictions are colour coded, where

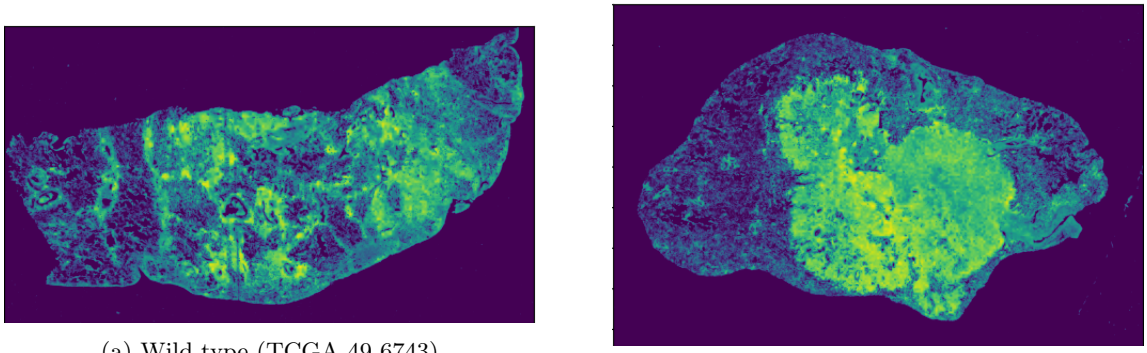

(a) Wild-type (TCGA-49-6743)

(b) TP53 Mutated (TCGA-L9-A444)

Figure 4: Mutation Status Prediction heatmaps of two LUAD Tumours

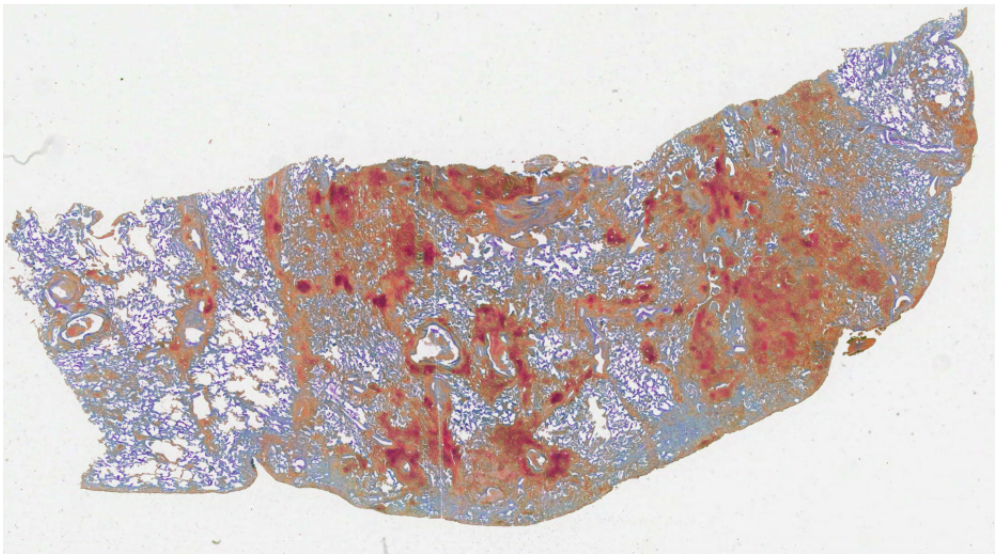

Figure 5: Wild Type LUAD tumour (TCGA-49-6743)

red means greater chance of mutation, and blue means lower chance of mutation. Note, the values have been scaled, so that we are able to differentiate between small differences in confidence of the model's predictions. For the two tumours shown, we see a large red patch in the mutated tumour, and smaller spread out red patches in the wild type tumour. While these results look promising, the model confience is still very low. Nevertheless, assuming we can train a better model, these visualisations will be very helpful to evaluate results, and potentially perform error analysis.

5 Deep Feature Extraction

I utilised the deep tissue extractor, from TIAToolbox to extract features at 1x magnification, for patches of size (256,256). This results in 36 patches and feature vectors for each WSI. I perform this for all 100 WSIs and save the raw features.

Next, I had to parse the feature vectors and positions of the patches into the format suitable for use with TripletMIL. This meant creating a dictionary of "filename" and "feature", where I created an artificial filename by adding the patient ID to the position values (e.g TCGA-L9-A444_250_0_500_250.jpg). I then used pickle to store the features in this form, and used TripletMIL to train on these features.

I adjusted the TripletMIL parameters to fit a 2048 input dimension, and point the program towards the location of my processed features. However, after trying features extracted at both 1x and 2.5x magnification, I was not able to get any good results. Nevertheless I performed inference on the test set, and plot the results. Since the prediction results in predicting all 0s or all 1s, the plots showed no results, and thus are not displayed here.

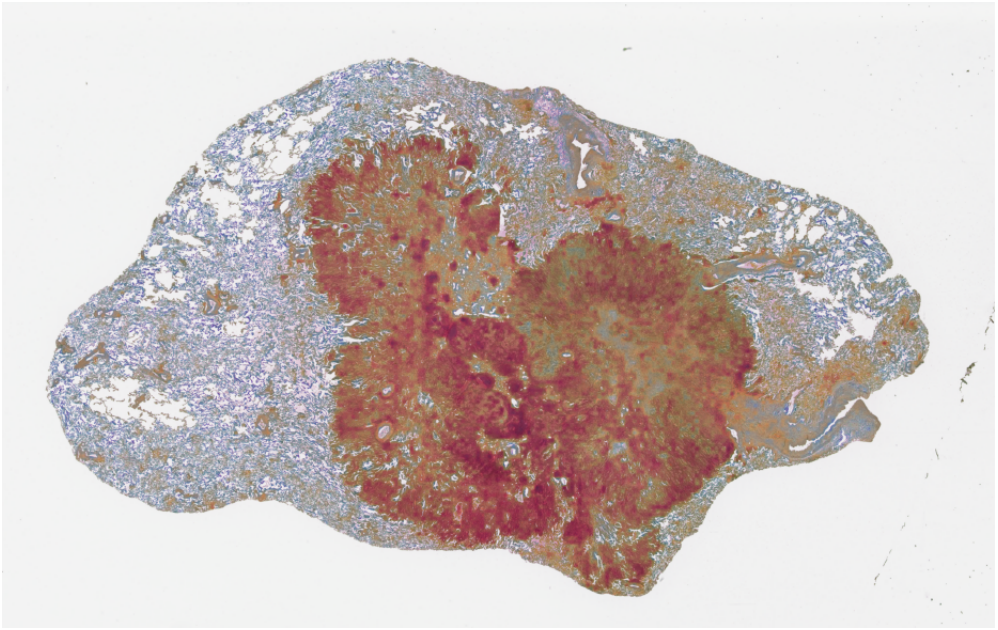

Figure 6: TP53 Mutated LUAD tumour (TCGA-L9-A444)

References

[1] J. Pocock, S. Graham, Q. D. Vu, M. Jahanifar, S. Deshpande, G. Hadjigeorghiou, A. Shephard, R. M. S. Bashir, M. Bilal, W. Lu, D. Epstein, F. Minhas, N. M. Rajpoot, and S. E. A. Raza, "TIA-Toolbox as an end-to-end library for advanced tissue image analytics," *Communications Medicine*, vol. 2, no. 1, pp. 1–14, Sep. 2022.

[2] R. Wang, S. A. Khurram, A. Asif, L. Young, and N. Rajpoot, "Rank the triplets: A ranking-based multiple instance learning framework for detecting HPV infection in head and neck cancers using routine H&E images," Jun. 2022.